

AD-A176 885

COMPARISON OF TEST STRUCTURES USED FOR THE MEASUREMENT
OF LOW RESISTIVE M. (U) STANFORD UNIV CA DEPT OF
ELECTRICAL ENGINEERING T SCHREYER ET AL. 1985

1/1

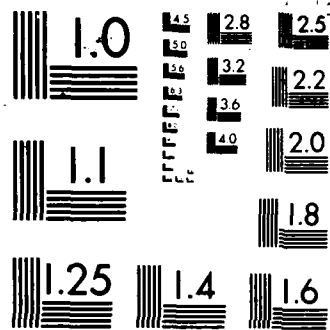
UNCLASSIFIED

DAAG29-85-K-0048

F/G 9/1

NL





MICROCOPY RESOLUTION TEST CHART
NATIONAL BUREAU OF STANDARDS 1963-A

Comparison of Test Structures used for the Measurement of Low Resistive Metal-Semiconductor Contacts

T. Schreyer, S. Swirhun, W. Loh, K. Saraswat and R. Swanson

Dept. of Electrical Engineering, AEL 2, Stanford University
Stanford, CA 94305.

Contract DAAG29-85-K-0048

(415) 497-1344

DTIC ELECTE
FEB 19 1987

ABSTRACT

Specific contact resistivity ρ_c ($\Omega\text{-cm}^2$), which can be extracted from measured contact resistance R_c (Ω), is a commonly used measure of metal-semiconductor contact quality. It is independent of current flow and contact geometry, and depends only on the transport properties of the metal to semiconductor junction. Unfortunately, extraction of ρ_c obtained from test structures differing in size or design often disagree by as much as an order of magnitude primarily because simple 1-D models which are used to extract the value of ρ_c can not account for fringing resistance associated with the 2-D nature of the current distribution around the contact [1]. For example, in a widely used model [2] for cross bridge Kelvin resistor the expression $\rho_c = (R_c \times \text{contact area})$ is used. But in practice, a sublinear behavior is often observed in a plot of ρ_c vs contact area, from which a meaningful value of ρ_c can not be extracted if this 1-D model is used, [3].

In this work we have used a 2-D simulator to analyze three commonly used contact resistivity measurement devices: the cross bridge Kelvin resistor, the transmission line tap resistor, and the contact end resistor, which are all shown in Fig. 1. This analysis was used to assess the extent of the error introduced by the use of 1-D models for extraction of ρ_c , and to develop a method by which a 2-D model may be used to extract a more reliable value. This method is then generalized so that a limited number of simulations may be used to extract ρ_c from devices with a wide variety of geometries and sheet resistances. The technique has been used to obtain ρ_c for PtSi, Pd₂Si, W and Al contacts to N⁺ and P⁺ Si with dopant concentration in the range of 10¹⁸ - 10²⁰ cm⁻³.

Fig. 2 shows the results of these simulations, where the Helmholtz equation $\nabla^2 V = V/(\rho_c/R_s)$ was solved in the contact region, and the Laplace equation was solved in the remainder of the diffusion region. For the ideal structures where the contact width is the same as that of diffusion ($\delta=0$) the conventional 1-D models shown in Fig. 1 give the same results as the 2-D models. However, for real structures with finite values of δ the measured values of the contact resistance (R_k , R_f and R_e for Kelvin, transmission line and end resistances, respectively) are significantly larger than the 1-D model prediction. This is due to the added voltage which is generated by current flowing in the overlap region between the contact and the diffusion edge. This effect becomes larger for lower ρ_c , higher δ and higher sheet resistance. Clearly the use of 1-D models will result in overestimation of ρ_c . This effect is most serious for the contact end resistance structure, and least serious for the transmission line tap structure.

By systematically varying either the diffusion width or the contact area the fringing parasitic resistance can be isolated from the true interface contact resistance by comparing the experimental data to 2-D simulations as shown in Fig. 3 for the cases of Kelvin and contact end resistance structures. By simulating the same device over a variety of resistivities, and by fitting the data points to one of the simulated curves, ρ_c can be determined. We have fabricated the three structures on the same test chip and demonstrated that the same value of ρ_c is obtained.

Unfortunately, this method requires a new set of simulations for each value of ρ_c and R_s . But by using the previously developed theory of scaling of contacts [1,4] we have determined that a more efficient extraction technique is to express the ratio R_c/R_s (where R_c is actually R_k , R_f , or R_e) as a single dimensionless parameter. This parameter is plotted against any appropriate

AD-A176 885

OFFICE COPY

This document has been approved for public release and sale; its distribution is unlimited.

geometrical variable, such as contact length or contact area, resulting in a set of universal curves which apply to a very wide range of ρ_c and R_c values. This method is illustrated in Fig. 4. and is applicable even to the "chain of contacts" structure, since that is simply a special case of the transmission line. If contact length and the parameter L_c are normalized to the overlap width δ , then these general curves will also apply to a wide range of contact and diffusion sizes.

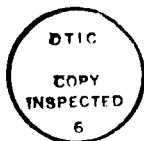
The curves shown in Fig. 2 reveal that of the three test devices simulated, the end contact resistor is the most sensitive to diffusion overlap δ . Varying this overlap from 0 to 2.5 microns can cause the contact resistance to vary by two orders of magnitude or more. Therefore this device cannot be relied upon to provide accurate estimates of ρ_c . Of the two remaining structures, the transmission line is the least sensitive to variations in geometry, but in practice it can be inaccurate, because of the diffusion leading up to the contact. Because this diffusion is part of the current path, and also part of the voltage tap, its resistance must be subtracted by extrapolation from the total measured resistance. This diffusion resistance can typically be 2 orders of magnitude larger than R_f , rendering the subtraction very unreliable. We would therefore recommend the cross-bridge Kelvin resistor as the most accurate of these structures, because it has a minimum parasitic resistance in its voltage tap, and is therefore relatively insensitive to variations in geometry. When used in conjunction with a 2-D model, it can provide very accurate results.

REFERENCES

- [1] W. Loh, K. Saraswat and R. Dutton, *IEEE Elect. Dev. Lett.*, vol. EDL-6, p. 105, 1985.
- [2] S. Proctor and L. Linholm, *IEEE Elect. Dev. Lett.*, vol. EDL-4, p. 294, 1982.
- [3] R. L. Maddox, *IEEE Trans. Elect. Dev.*, vol. TED-32, p. 682, 1985.
- [4] W. M. Loh et al, *IEDM Technical Digest*, pp.586-589,1985.

Approved for	
Dissemination	
Classification	
Justification	

By	
Distribution	
Availability Code	
Symbol	
Date	



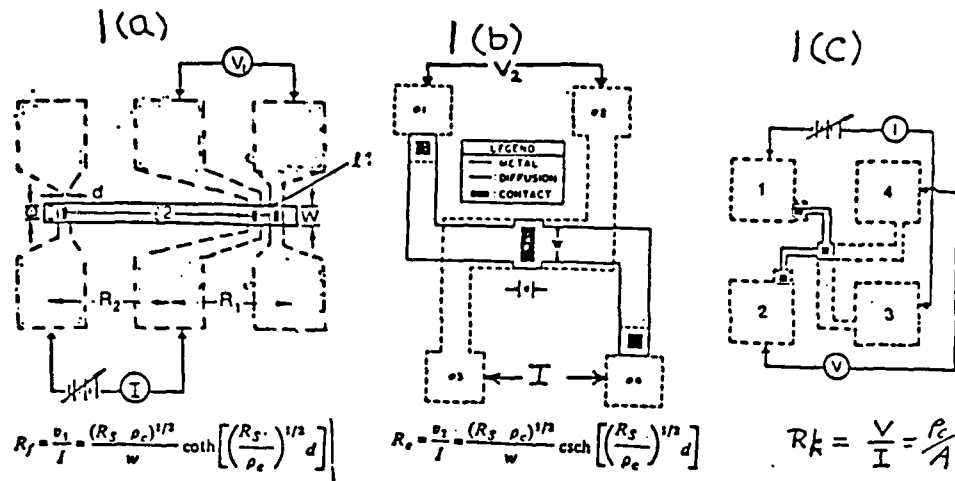


Fig 1. Test structures for contact resistance measurements along with 1-D model expressions: (a) transmission line, (b) end contact and (c) cross bridge Kelvin resistance structures.

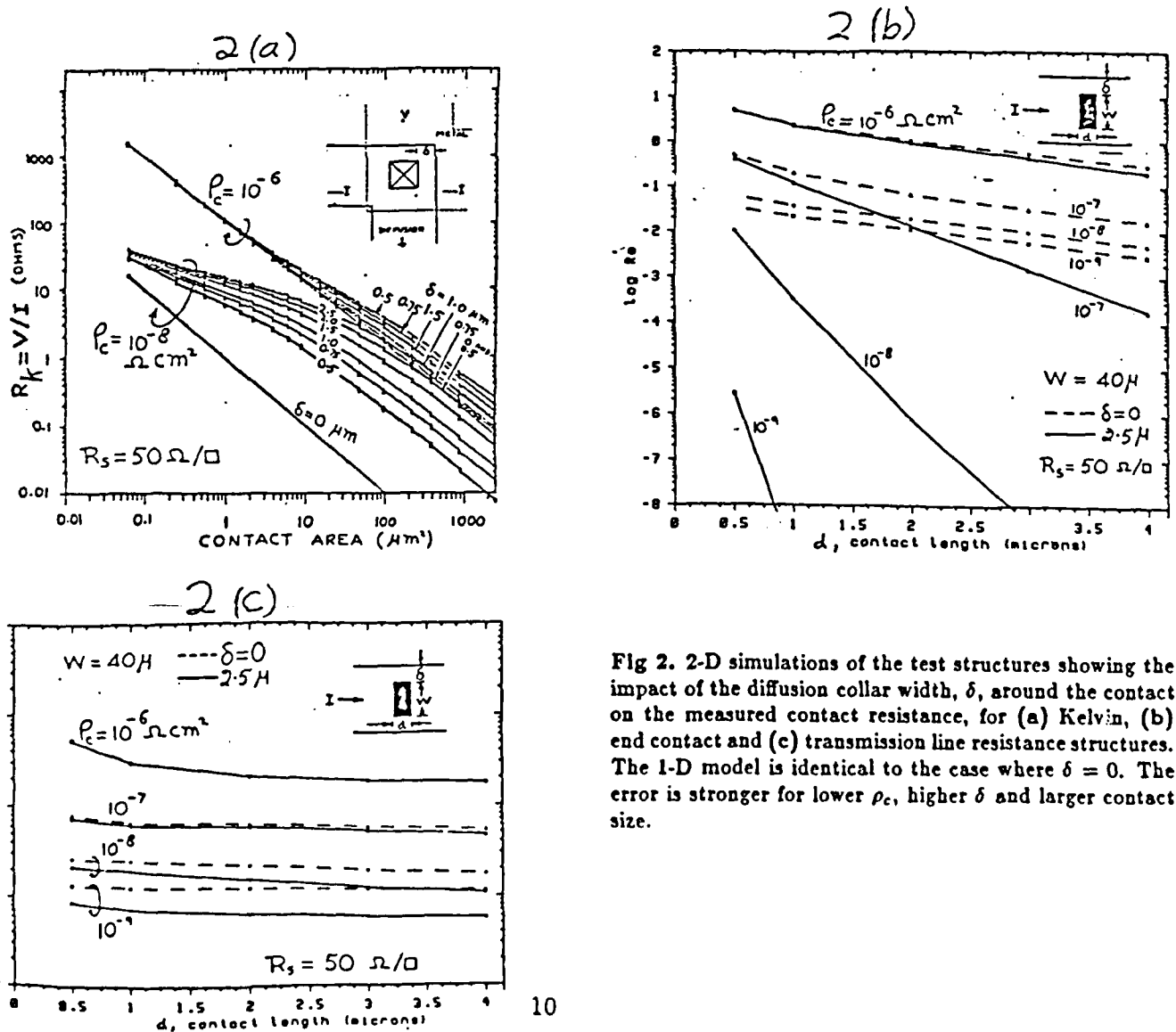


Fig 2. 2-D simulations of the test structures showing the impact of the diffusion collar width, δ , around the contact on the measured contact resistance, for (a) Kelvin, (b) end contact and (c) transmission line resistance structures. The 1-D model is identical to the case where $\delta = 0$. The error is stronger for lower ρ_c , higher δ and larger contact size.

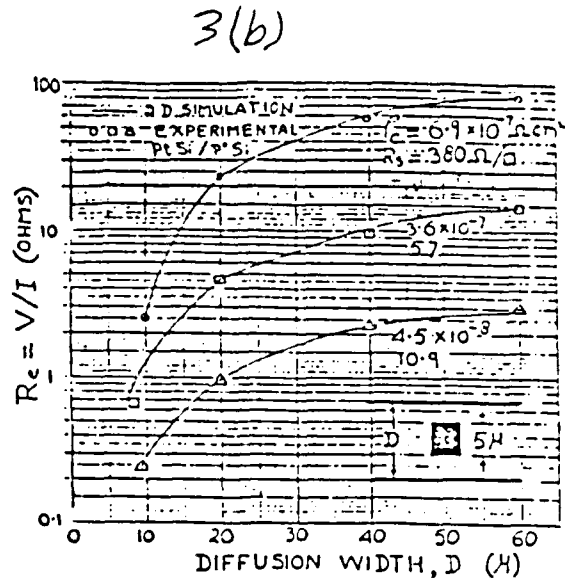
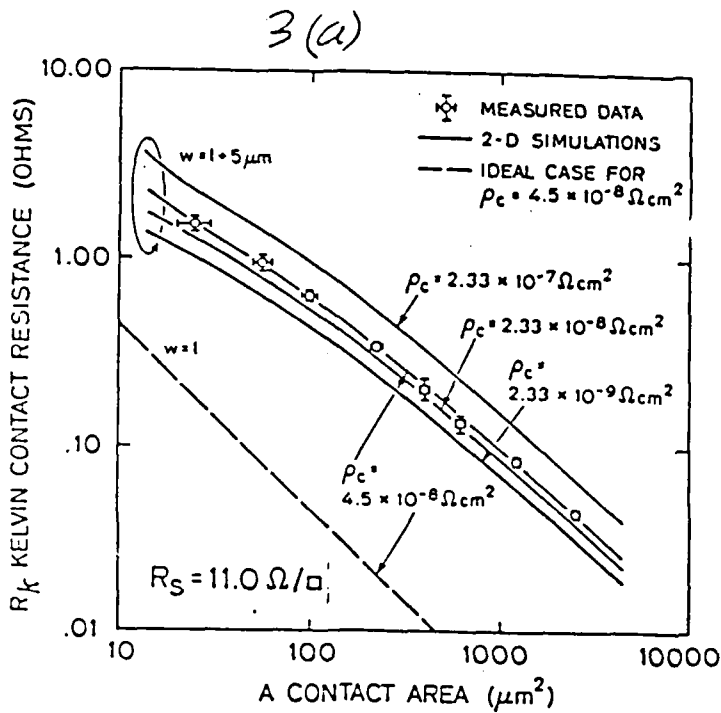


Fig 3. Illustration of the method used to extract ρ_c by plotting R_c data against geometry and fitting the data to the nearest simulation curve for (a) Kelvin resistance and (b) end contact resistance structures. The dashed line in part a shows the resistance given by the 1-D model for Kelvin resistance.

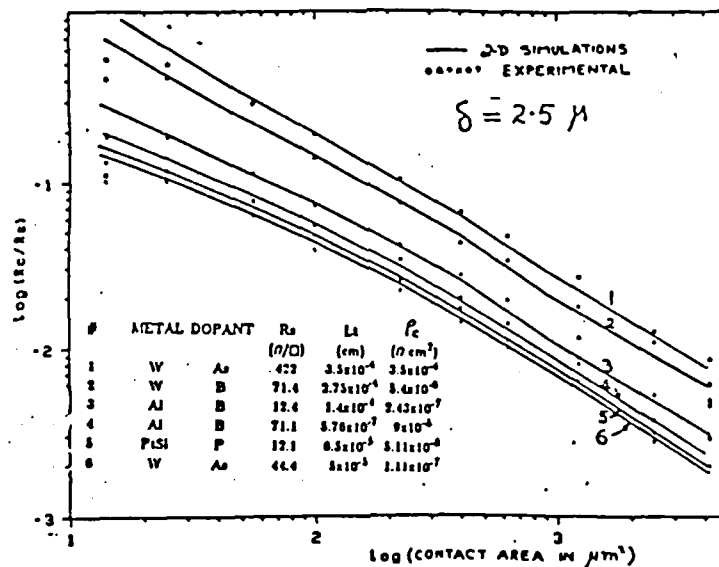
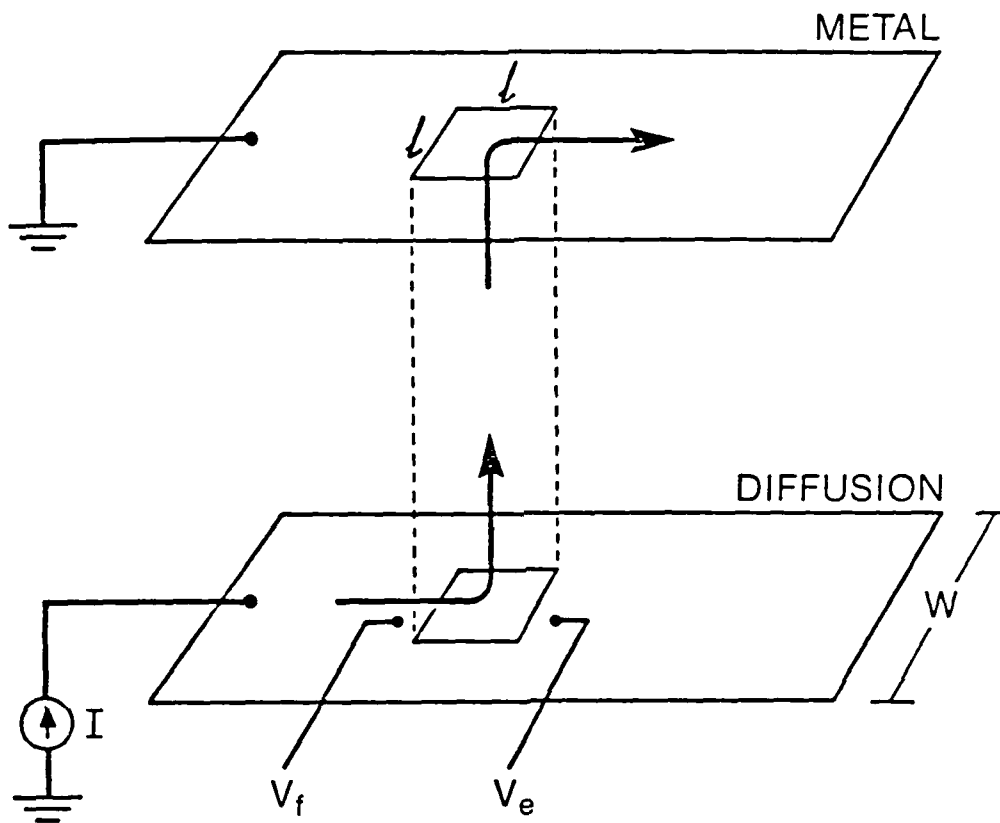


Fig 4. Generalized technique of ρ_c extraction for the Kelvin resistor structure by comparing the experimental data with a universal plot of R_c/R_s vs contact area as a function of transfer length ($L_t = \sqrt{\rho_c/R_s}$).



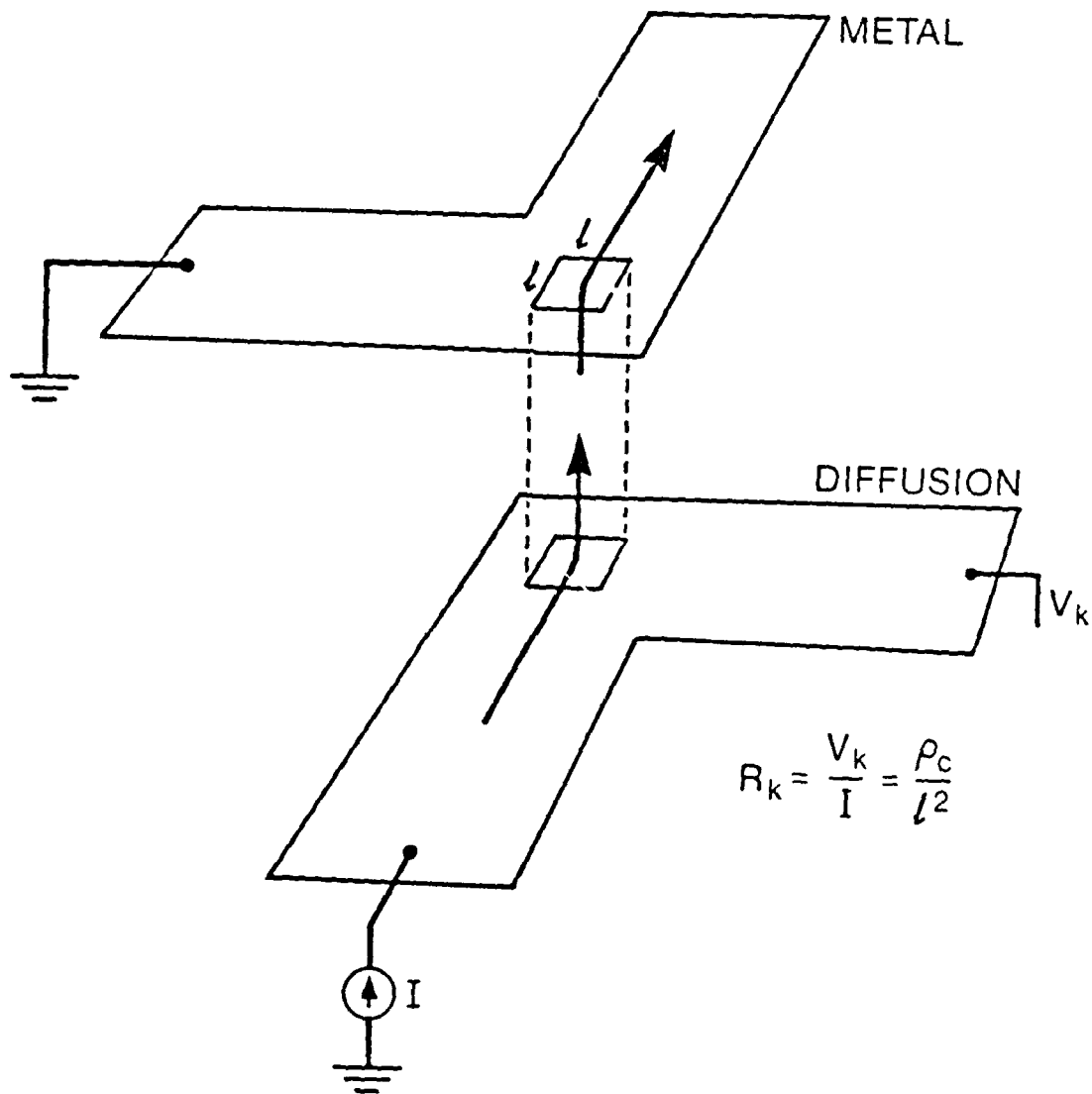
$$l_t \triangleq \sqrt{\frac{\rho_c}{R_s}}$$

$$R_e = \frac{V_e}{I} = R_s \frac{l_t}{W \sinh(l/l_t)} \quad \text{Contact End}$$

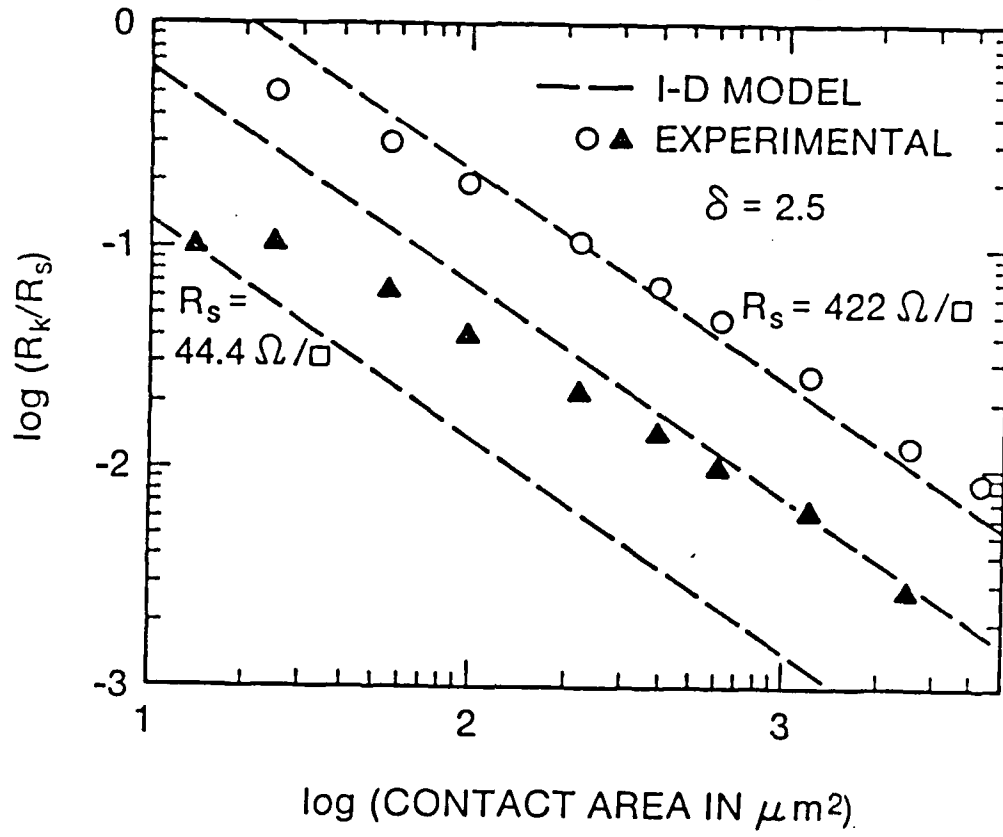
$$R_f = \frac{V_f}{I} = R_s \frac{l_t}{W \tanh(l/l_t)}$$

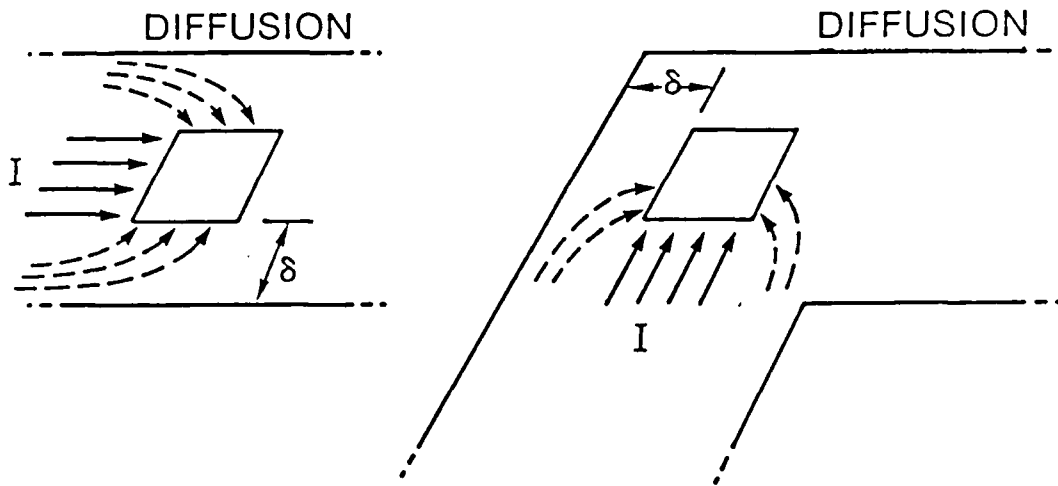
Transmission Line Tap

Cross Bridge Kelvin Resistor

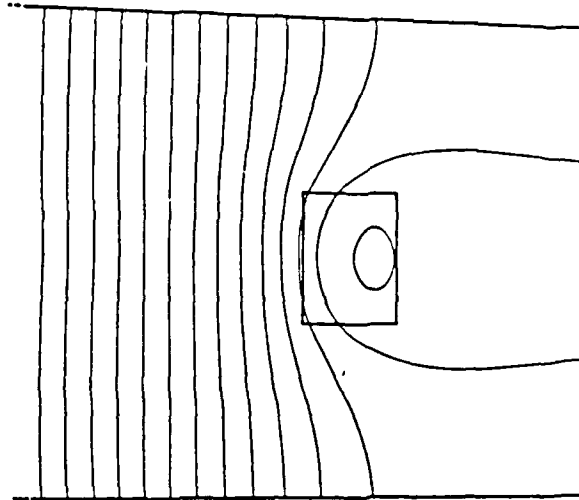


W TO As-DOPED Si CONTACTS



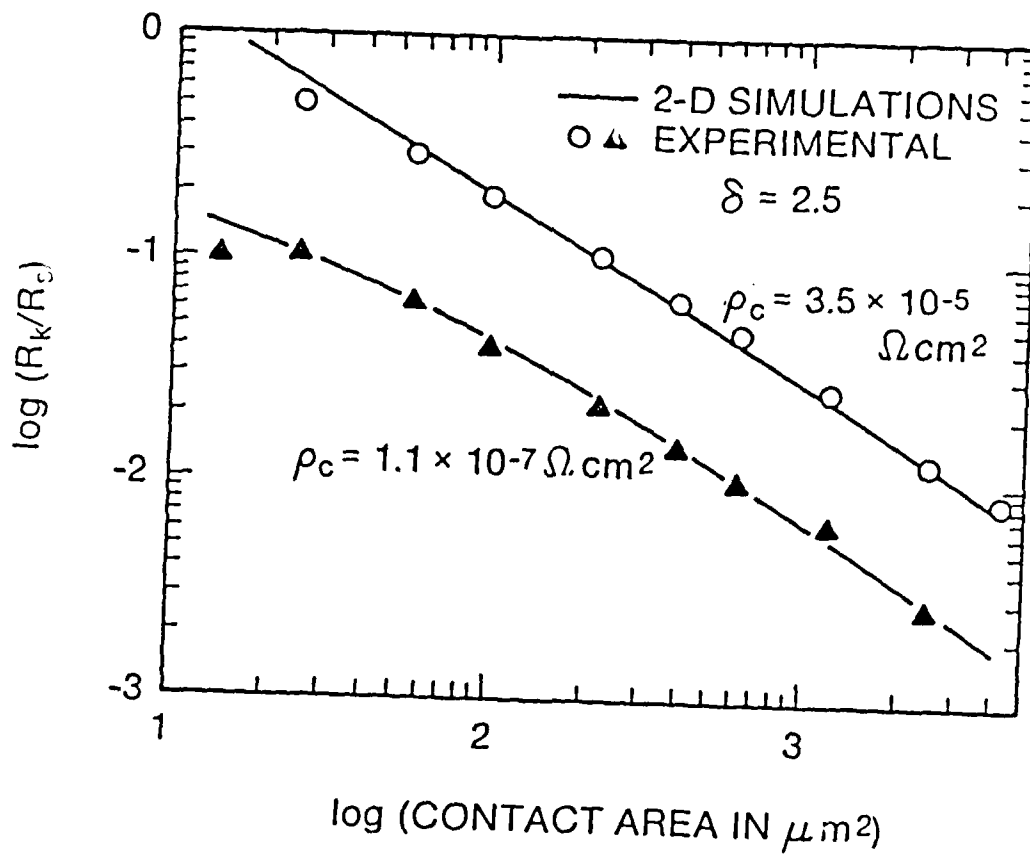


2-D Model of Metal/Diffusion Contact

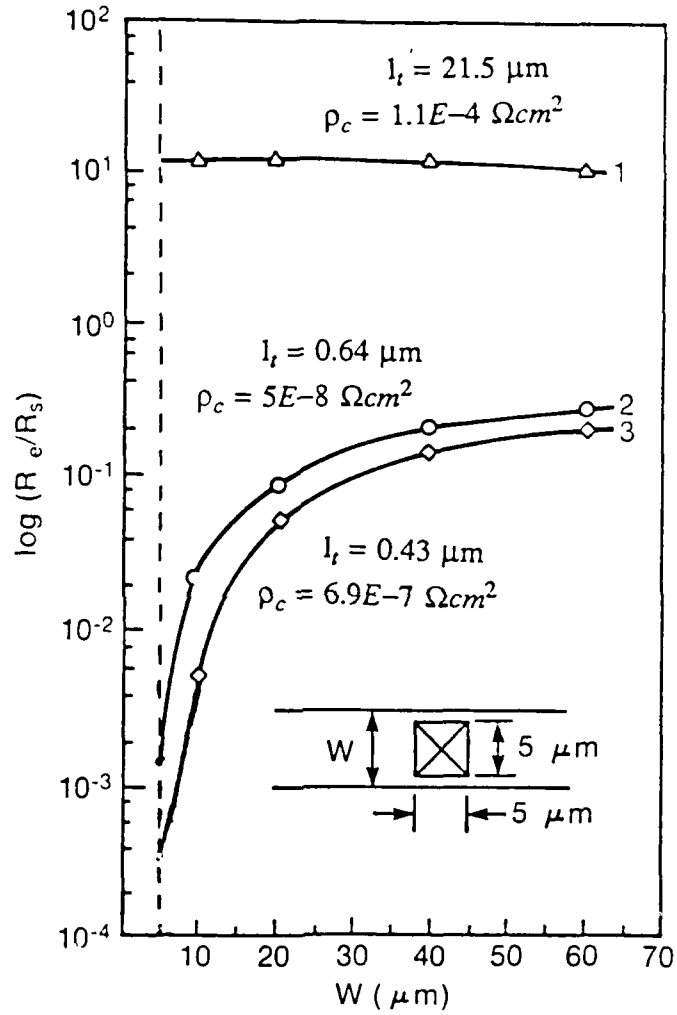


- $R_{Metal} \ll R_{Diffusion}$
- variation in depth ignored
- system described by potential in diffusion 'sheet', V
- $l_t = (\rho_c / R_s)^{1/2}$
- $\nabla^2 V = V/l_t^2$ underneath contact
- $\nabla^2 V = 0$ elsewhere
- measure potential V^*

$$\frac{R^*}{R_s} (l_t) = \frac{V^*}{\int_{d_1} \frac{\partial V}{\partial x} dy}$$



Contact End Resistor

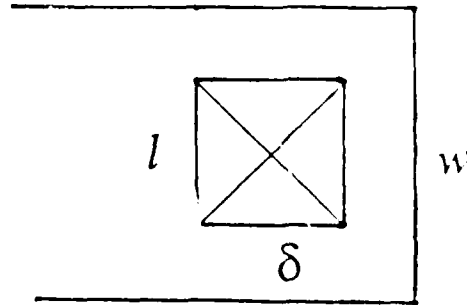


Universal Curves from Scalings

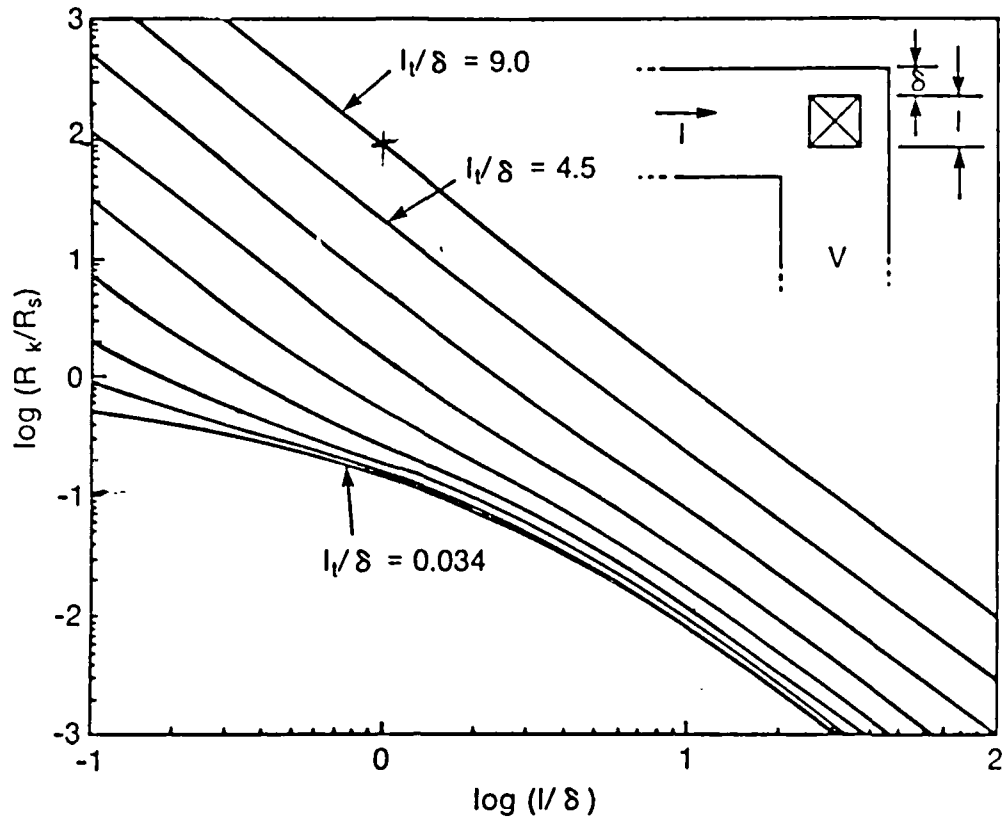
- $\nabla^2 V = V/l_t^2$ underneath contact
- $\nabla^2 V = 0$ elsewhere
- $l_t = (\rho_c / R_s)^{1/2}$
- linearity of equations implies:

$$\frac{R^*}{R_s} (l, w, l_t) = \frac{R^*}{R_s} \left(\frac{l}{L}, \frac{w}{L}, \frac{l_t}{L} \right)$$

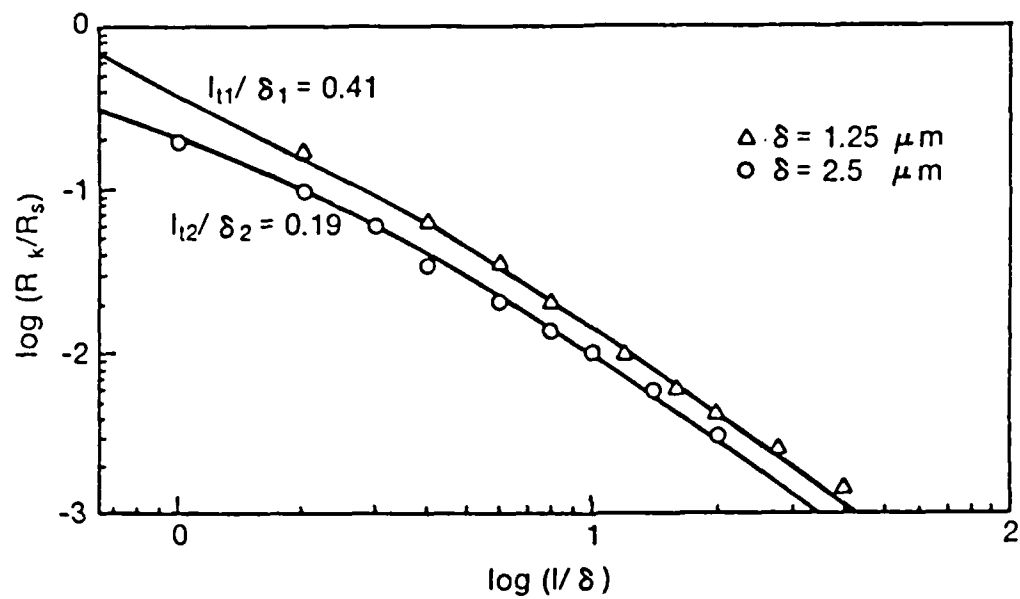
- choose $L = \delta$



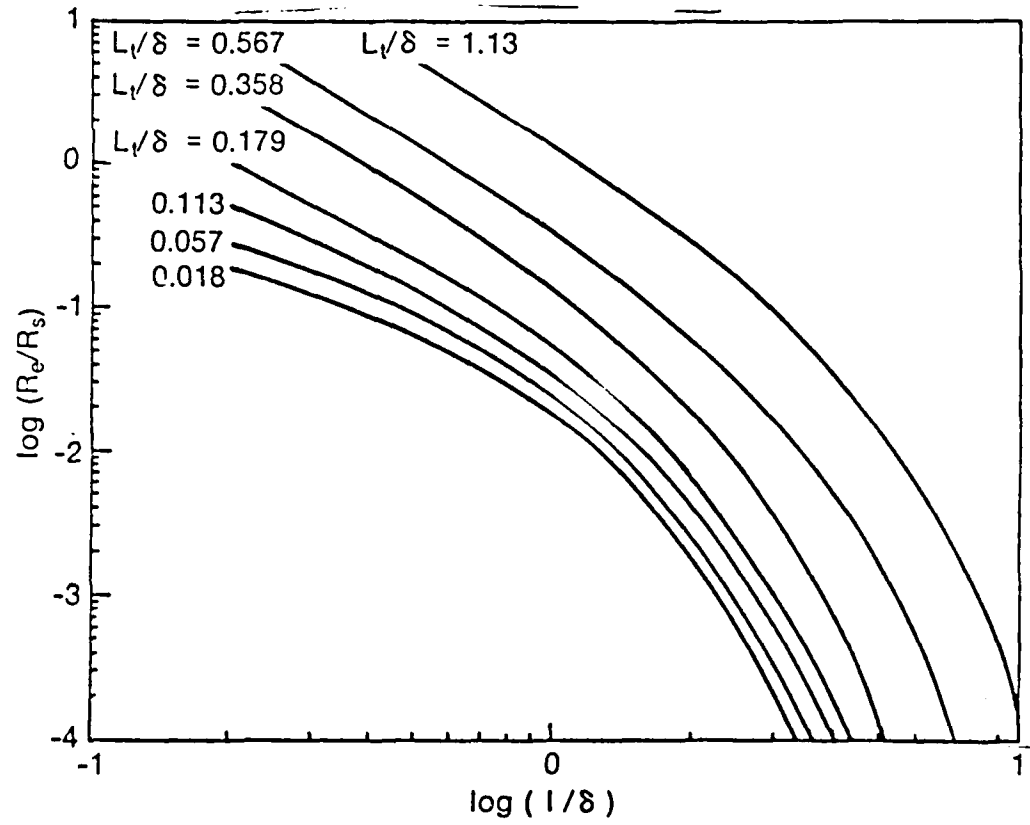
Cross Bridge Kelvin Resistor



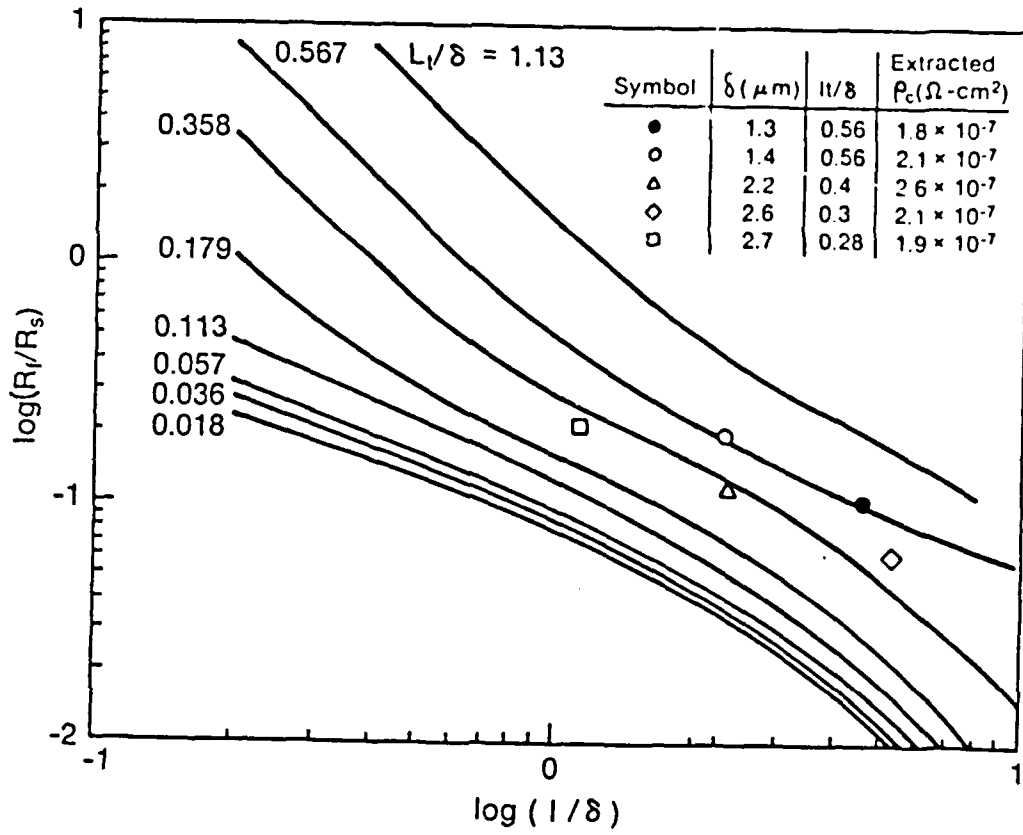
Cross Bridge Kelvin Resistor



Contact End Resistor



Transmission Line Tap



END

3-87

DTIC